Mechanics and Mechanical Engineering
Vol. 20, No. 1 (2016) 43–57

The Analysis of the Cutting Forces and Surface Layer Stereometry in the Grinding Process of Abrasion–Resisting Materials

Ryszard Wójcik
Anna Grdulska
Radosław Rosik
Przemysław Wejman
Institute of Machine Tools and Production Engineering
Lodz University of Technology
Stefanowskiego 1/15, Łódź, Poland
ryszard.wojcik@p.lodz.pl
grdulska.anna@gmail.com
radoslaw.rosik@p.lodz.pl
przemyslaw.wejman@gmail.com

Received (20 January 2016)
Revised (26 January 2016)
Accepted (11 February 2016)

The article presents the investigation of the grinding process of flat samples made of materials that meet requirements of the lowest abrasibility, which belong to difficult to machine materials. Research enclosed measurement of cutting forces and surface layer stereometry during grinding without using cutting fluid. The tests were carried out with the aid of new generation grinding wheel, Quantum.

Keywords: Quantum, wear, XAR 400, Brinar 400, Dillidur 500V, grinding.

1. Introduction

There is a big variety of the materials used in surface mining. They can be characterized by diversified utility properties or abrasive wear, the proper level of safety as well as and environment protection [2, 7]. Among the most important aspects that have a decisive influence should be replaced strength and tensile resistance at extreme temperatures [2, 7]. They must ensure the trouble-free plastic working both cold and hot working, bearing in mind mechanical processing [1, 10].

The process of surface layer shaping has a vital importance on the final work results of steels used in those areas of the economy [4, 7]. In processes involving grinding important issue is the use of cutting fluids, which are designed to reduce friction, and thus the temperature of the process [2, 3, 7].

The parameters describing the wear resistance of the material are hardness of

abrasive material T_o (HV) and the hardness of the grinded material Tm (HV). Where the relative durability T_w [9, 10] is described by the formula

$$T_w = T_o - T_m \tag{1}$$

Wear resistance of the actual conditions depends on several factors:
- Forces which influence on the surface of the material.
- The speed and the size of the particles acting on the surface material.
- The direction of the surface of the material.
- The percentage of the individual components forming the abrasive environment.

In most industrial applications of these factors combined with each other they compose a combination leading to different levels of resistance. In some cases, to achieve high strength in combination with wear resistance requires a martensitic structure. On the other hand getting strength, hardness and toughness requires a phase structure: bainite, ferrite, pearlite coagulated. Because of this there are required technologies to provide high utility value and quality. Fig. 1 presents an exemplary construction of the abrasive material which is a mixture of different abrasive materials with different hardness and with proper percentage participation.

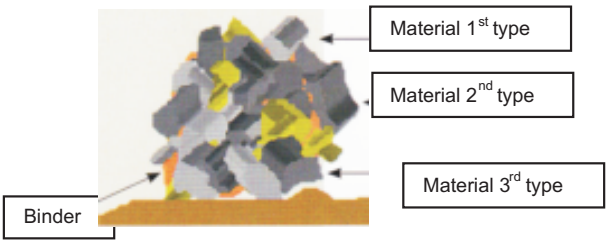

Figure 1 Structure of abrasive affecting the abrasion–resisting materials

It means that in case of the parameter T_o is equal to the sum of the percentage products of the individual solid components of material that compose in the structure of the grinded material.

Equivalent hardness of the abrasive material equals:

$$T_o = (\%)_1 \cdot T_1 + (\%)_2 \cdot T_2 + (\%)_3 \cdot T_3 \tag{2}$$

where:

$(\%)_{1,2,3}$ – the percentage of the individual components of abrasive material,

$T_{1,2,3}$ – hardness of each materials.

Destruction of abrasive materials is caused by many factors, both mechanical, strength or chemical. In Fig. 2 they have been taken into account [5, 8, 10].

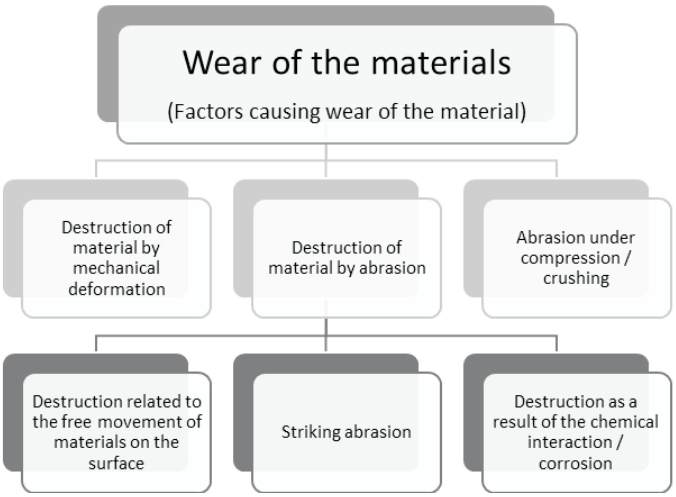

Figure 2 Factors causing wear of the grinded materials [9, 10]

The processes of wear materials may be caused by the deformation, induced by the cutting process, described as D – type 1 (Fig. 3a) and D – type 2, associated with the processes of plastic flow (Fig. 3b).

In turn, the relative vitality Z_w is a parameter that defines resistance of the material on the surface deformation. They are associated with the impact of the abrasive material on the surface layer (SL). Relative vitality involves the relation between the different types of deformations.

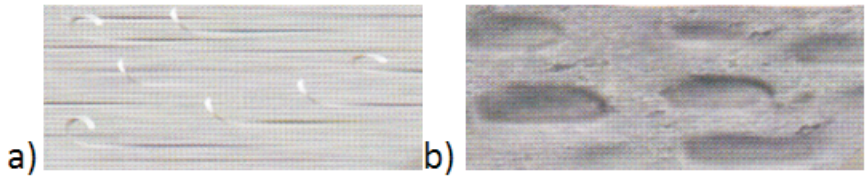

Figure 3 Types of surface deformation of the material during abrasion: a) D – type 1, b) D – type 2

Each of the presented deformation shortens the life of the relative area. In fact, it takes into account the resistance to: tangential friction, striking abrasion and abrasion caused by the compression. Tab. 1 summarizes the abrasive processes with the appropriate numerical coefficients and an indication of their level.

Thus, depending on the composition of abrasive material and the percentages of the various fractions, the course and form will be different. As an example is presented percentages of ingredients typical abrasive materials that are found in different natural conditions occurring in surface mining:

Table 1 Abrasion Resistance [9, 10]

Tangential friction	Percussive abrasion,	Abrasion caused by compression	Type abrasion resistance
T_w >1,8 (D – typ 1)	T_w >1,2 (D – typ 1)	T_w >1 (D – typ 1)	Low
1,8>T_w >1,5 (D – typ 1 i 2)	1,2>T_w >0,8 (D – typ 1 i 2)	T_w ∼1 (D – typ 1 i 2)	Medium
T_w <1,5 (D – typ 2)	T_w <0,8 (D – typ 2)	T_w <1 (D – typ 2)	High

Sand – quartz 50% - 98%

Apatite – 61% quartz, 11% alumina, limestone 6%

Basalt – 40% quartz, alumina 11%, limestone 14%

Tab. 2 shows the average hardness [HV], the selected materials only.

Table 2 Materials hardness [9, 10]

Material	The average hardness [HV]
Fluorite	150
Apatite	360
Quartz	1070
Corundum	1860

Among the many wear resistant materials used in the industry was selected: XAR 400 Brinar 400 Dillidur 500V. Tab. 3 presents the chemical composition of the particular steels that tests have been carried out.

2. Preparation for testing

The process of surface grinding were carried out on a grinding machine SPD - 30b, by means of the grinding wheel 01 350x32x127 2NQ 60J VS3, and without using cutting fluid. The research was carried out with the following parameters: v_w = 0.2 m / s, v_s = 25 m / s, a_{e1} = 0.01 mm and a_{e2} = 0.02 mm. During the investigations the following samples materials were used XAR 400, Brinar 400 and Dillidur 500V, uncase-hardened due to carbon content of about 0.3%. The dimensions of samples: 10x30x100 mm. Single–pass grinding process was employed to determine the course of force components for certain allowances. During the tests grinding force components: tangential Ft and normal Fn were measured by using dynamometer Kistler type 5019. The signal from dynamometer was sent to an amplifier type 5011, then into a data acquisition module type kusb–3108 Keithley (USA) and finally processed by means of software quick DAQ.

Table 3 The chemical composition of tested steels [7, 9, 10]

Steel name	Chemical composition %								
	C	Si	Mn	P	S	Cr	Mo	Ni	B
XAR 400	0,2	0,8	1,5	0,02	0,02	1,0	0,5	-	0,01
Brinar 400	0,18	0,3	1,5	0,01	0,00	1,4	0,6	-	-
Dillidur 500V	0,3	0,3	1,8	0,03	0,01	1,5	0,5	1,0	0,01

Table 4 Mechanical properties of tested steels [9, 10]

Steel Name	Steel No	R_e [MPa]	R_m [MPa]	A%	HB
XAR 400	1.8714	1050	1250	12	360-440
Brinar 400	1.8715	1100	1300	12	340-440
Dillidur 500V	1.8721	1300	1650	8	450-530

3. Results of study

Fig. 4 is presenting the test results obtained by grinding steels Brinar 400 (Fig. 4a), Dillidur 500V (Fig. 4b) and XAR 400 (Fig. 4.c). Parameters of the grinding process were given before, allowance $a_e = 0.02$ mm. For the first two materials the stability of the grinding process wasn't reached. At the entrance into the material force components increased, in the central part of the length of the sample forces reduced. The highest values of the force components were achieved for the material XAR 400 (Fig. 4c).

Fig. 5 collates data from plunge grinding processes of three steels, a depth of cut $a_e = 0.01$ mm, other parameters the same as in the previous tests.

For all tested materials obtained much lower grinding force components – a decrease approximately 50% for the depth $a_e = 0.01$ mm. Values of force components during concurrent and backward grinding of the surfaces are shown in Fig. 5: a) Brinar 400, b) Dillidur 500V, c) XAR 400. Higher values of force components were obtained for the material Brinar 400. For all workpiece materials maximum force level achieved in the middle of the sample.

4. Surface roughness measurement

To measure the surface topography profilograph Hommel Hercules Werkzeughandel model TurboWaveline60 was used. Measuring position is shown in Fig. 6. Profilograph TurboWaveline60 with dedicated software enables the measurement roughness and waviness of the samples. By using a special software Hommel Map based on a given number of passes of the measuring needle is created a spatial topographic map of the tested surface in 3D system.

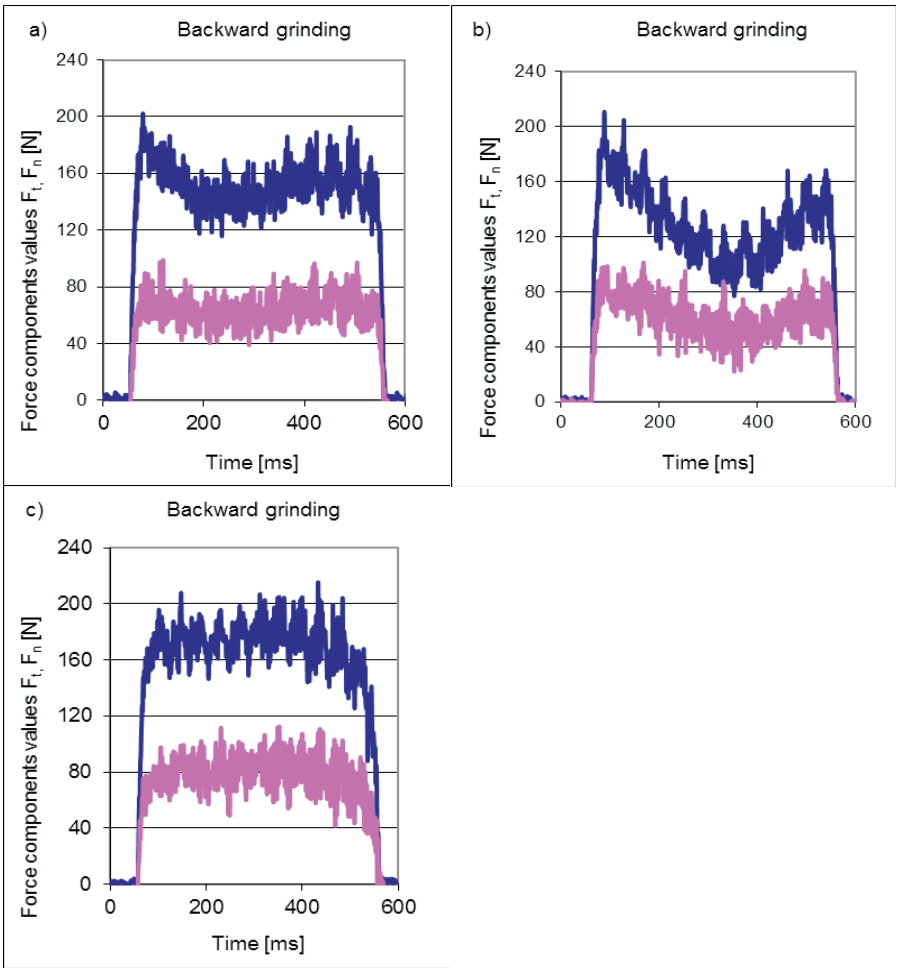

Figure 4 Force components surface grinding, while single–pass grinding backward: a) Brinar 400, b) Dillidur 500V, c) XAR 400

Table 5 The mean value of the force component

Steel Name	The mean value of the force component F_n	The mean value of the force component F_t
XAR 400	120 N	80 N
Brinar 400	154 N	80 N
Dillidur 500V	120 N	76 N

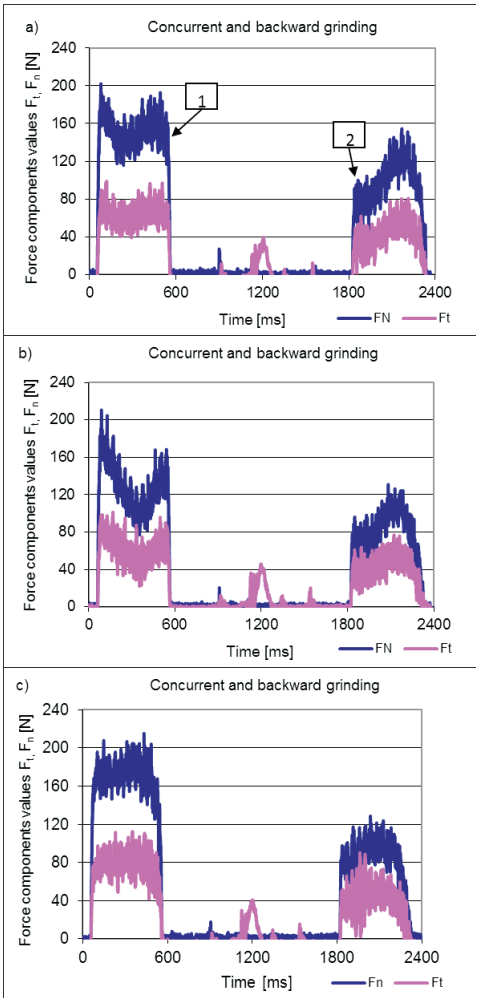

Figure 5 Values of force components during concurrent (1) and backward (2) grinding flat surfaces: a) Brinar 400, b) Dillidur 500V, c) XAR 400

5. Results of surface layer stereometry

Tab. 6 shows the values of the SGP parameters of the grinded samples surface layer made of abrasion–resisting materials. They enclose selected parameters of the geometrical surface structure: amplitude, surface and volumetric, spatial, hybrid and functional.

Data presented in Fig. 7 shows that depending on the type of grinded material the distribution of the material at the height of the profile (distribution function ADF) and the shape of spatial curve the participation of the material are changing. Grinding Dillidur 500V (Fig. 7b) causes that much more material accumulates within the hills or over the line average, which may indicate the deformation of the profile.

Figure 6 Measuring position- Profilograph TurboWaveline60

Table 6 Parameters of the geometrical surface structure

Parameter sign	Surface		
	Materials		
	Binnar 400	Dillidur 500V	Xar 400
Amplitude parameters			
Sa	0,184 μm	0,206 μm	0,185 μm
Sq	0,234 μm	0,289 μm	0,243 μm
Sp	1,170 μm	4,810 μm	3,350 μm
Sv	1,16 μm	1,33 μm	2,09 μm
St	2,33 μm	6,13 μm	5,44 μm
Ssk	0,0294	1,73	-0,0478
Sku	3,56	26,5	5,73
Sz	1,94 μm	4,68 μm	3,61 μm
Spacial parameters			
Sds	25,6 pks/mm^2	28 pks/mm^2	28,6 pks/mm^2
Str	0,0229	0,0182	0,0082
Sal	2,68x10^{-5}mm	2,13x10^{-5}mm	9,62x10^{-6}mm
Hybrid parameters			
Sdq	0,039 μm/μm	0,0512 μm/μm	0,0585 μm/μm
Ssc	0,0165 1/μm	0,0242 1/μm	0,0244 1/μm
Sdr	0,0765%	0.129%	0.141
Functional parameters [mm^3/mm^2]			
Vmp	0,000157	0,000178	0,000246
Vmc	0,000838	0,000952	0,000149
Vvc	0,000274	0,000289	0,000267
Vvv	2,74x10^{-5}	3,43x10^{-5}	3,25x10^{-5}

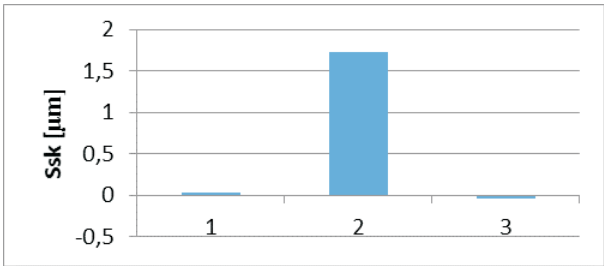

Figure 7 The value of the surface skewness Ssk: 1 – Brinnar 400, 2 – Dillidur 500V, 3 – Xar 400

The results of changes in the distribution of the material at the height of the profile are suitable modifications Ssk skewness (Fig. 8) a significant increase of parameters $S_{sk} = 1.73$ and $S_{ku} = 26.5$, what occurs during grinding Dillidur 500V.

Considering the shape of the curve of load capacity (8d BAC), it can be said that machining abrasion–resisting materials: Brinnar Xar 400 and 400 by means of a grinding wheel Quantum generally improves the load capacity of surface after grinding process.

6. Functional characteristic of the surface

Functional analysis is based on four volume parameters from the 13 V- parameters [2, 3, 9]:

– The volume of the core (V_{mc})
– Void volume in the core (V_{VC})
– The volume of material peaks (V_{mp})
– The volume of voids in the valley (V_{vv}).

The distribution for the above–mentioned materials are shown in Fig. 9. The largest void volume in the valley obtained after the grinding process of Dillidur 500V, V_{vv} = 3,43x10-5 mm^3 / mm^2. This increases the efficiency of fluid flow in the valley of roughness in the zone below the core [4]. In addition, the surface has a large number of voids of the core V_{vc} = 0,000289 mm^3 / mm^2, and therefore has a greater ability for collecting liquid in the core. This is a fundamental part of the surface height from the point of view of wear during utilization. The lowest value of the presented parameters obtained after grinding Brinnar 400. Additional data of fluid retention in the valleys of micro–ridges on the contact between two surfaces can be achieved on the basis of vectorization of the micro–grooves network [7].

7. The spatial and hybrid parameters

A collection of 12 S–parameters comprises four spatial parameters that describe the qualities the surface structure of [1, 4]:

– Fastest decay autocorrelation length (S_{al})
– Texture aspect ratio (S_{tr})
– Texture direction (S_{td})
– Peaks density (S_{ds}).

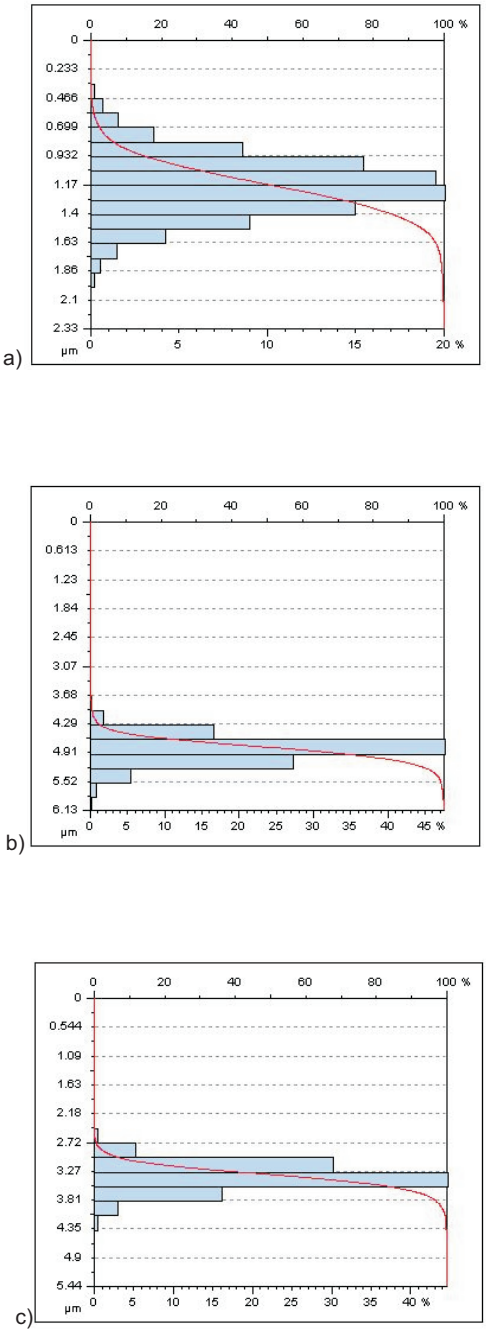

Figure 8 The shape of the curves participation of the material and distribution of ADF functions of the surface: a) Brinnar 400, b) Dilidur 500V, c) XAR 400

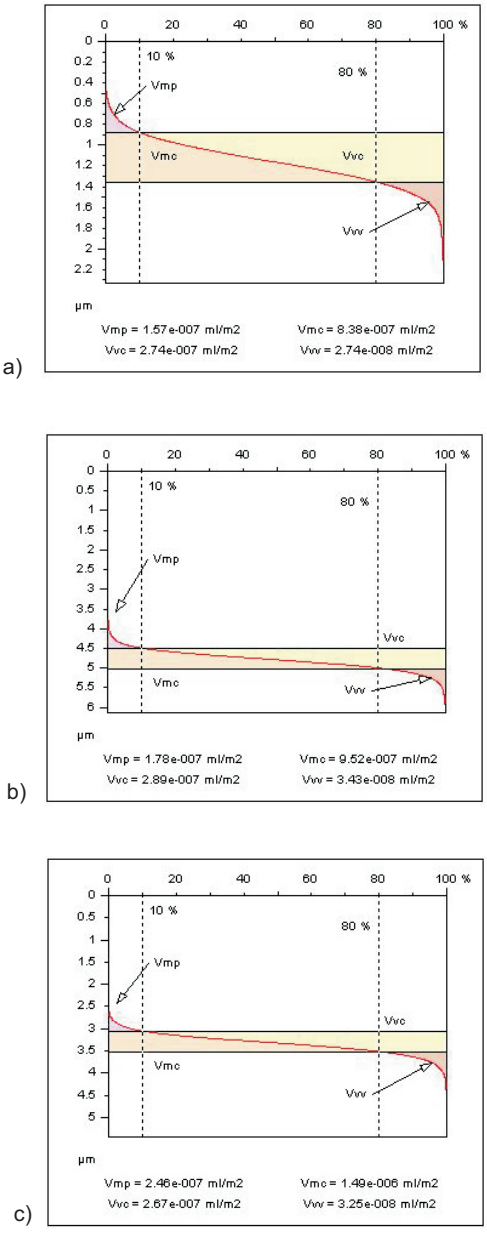

Figure 9 The volumetric functional parameters of the grinded surface:a) Brinnar 400, b) Dilidur 500V, c) XAR 400

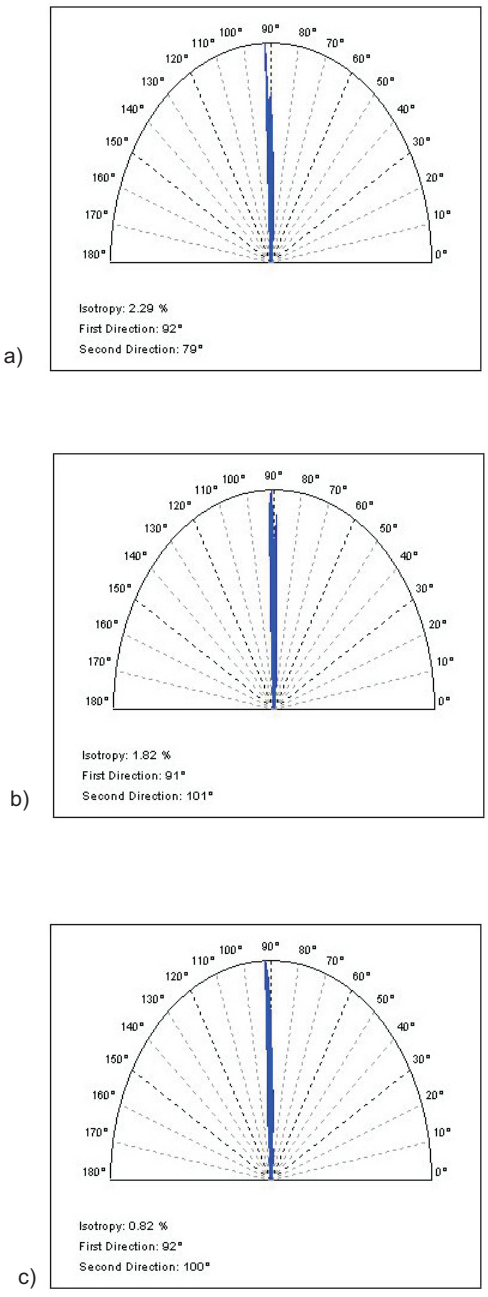

Figure 10 Directivity of the structure: a) Brinnar 400, b) Dilidur 500V, c) XAR 400

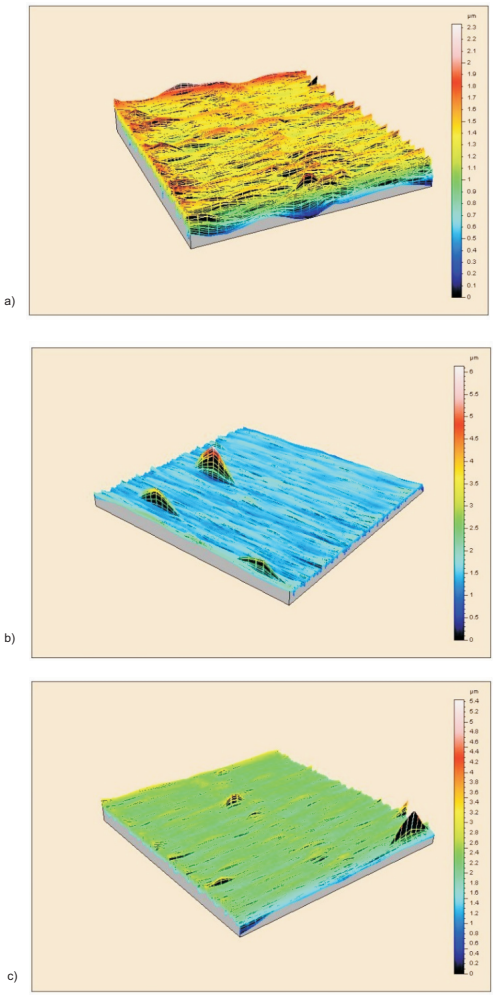

Figure 11 Distribution of the autocorrelation function for surfaces: a) Brinar 400, b) Dillidur 500V, c) XAR 400

The surfaces of materials Dillidur 500V and 400 XAR after grinding with depth of cut $a_p = 0.01$ mm contain much more peaks per unit area than after machining Brinnar 400. However, when the same material has a larger value of Str it means that the grinded surface has a poorer lay texture (i.e. anisotropy) from other workpiece materials. Nevertheless, the value of the parameter $S_{tr} < 0.1$ still indicates a high anisotropy of all the grinded surface.

These properties are confirmed by surface lay diagram that is shown in Fig. 10. As can be seen, the level of isotropy of Brinnar 400 slightly exceeds 2%. S_{td} and S_{al} parameters are the results of the analysis of the autocorrelation function and depend on surface stereometry. The value of the parameter S_{td} for Brinnar 400 and

XAR 400 equals 92^o, while for Dillidur 500V reaches 91^o for grinded surface. The value of this parameter indicates that the dominant cutting marks are perpendicular to the measuring direction. The greatest decay autocorrelation length S_{al} of the material was obtained for Brinnar 400 (Fig. 10a).

Whereas, on Fig. 11a and b can be seen that after grinding XAR 400 and Dillidur 500V have occurred local valleys. Proper chip evacuation zone to fast gumming up of grinding wheels grinding wheel hasn't exist. This adverse effect causes that, apart from cutting by means of abrasive grains, during the process further contact with the workpiece material have glued chips, which often extend beyond the contour of the wheel. Consequently, during machining they leave a trail of deep scratches on the surface.

Further in the paper were taken to analyze the next three hybrid parameters:

- Root Mean Square (RMS) Surface Slope comprising the surface, evaluated over all directions (S_{dq}),

- Mean Summit Curvature for the various peak structures (S_{sc}),

- Developed Interfacial Area Ratio (S_{dr}).

The surface of XAR 400 is composed of the roughness with a larger inclination ($S_{dq} = 0.0585$) than after machining Dillidur 500V ($S_{dq} = 0.0512$) and Brinnar 400 ($S_{dq} = 0.039$). Also the curvature for the various peak structures are bigger while grinding XAR 400 ($S_{sc} = 0.0244$) than other materials. S_{sc} parameter values are in the range of 0.004 – 0.03 μm-1, which is the typical value for the surface shaped by grinding. A positive feature of surface Brinnar 400 is also the smallest unit of $S_{dr} = 0.0765\%$.

8. Summary

The study contained the grinding process by means of the grinding wheel Quantum Vitrium3 without application of cutting fluid. After observation under the microscope the state of surface weren't found any damage to the surface layer in the form of burns or microcracks. Considerably smaller force components were obtained during grinding with smaller allowances, which is understandable. As a consequence of that, the less heat is cumulated in the grinding zone. It is associated with the fact that the wheel removes much smaller allowances.

Further research will include the grinding processes involving cutting fluid given in two different methods: flood method by means of MQL method into the cutting zone. The paper presents the results of the research involving only selected parameters of a profile characteristics and surface topography that were obtained while grinding samples made of difficult to machine materials: Brinnar 400, Dillidur 500V and XAR 400. The useage of different measurement techniques and visualization of the surface enables the assessment of stereometric features and exploitation properties. The rapid development of measurement technologies, make it possible to forecast the properties of functional of the elements, through proper selection of grinding conditions at various stages of the process.

References

[1] **Adamczak, S.**: Pomiary geometryczne powierzchni. Zarysy kształtu, falistość i chropowatość, *WNT* (in Polish), Warsaw, **2008**.

[2] **Burakowski, T. and Napadłek, W.**: Zarządzanie technologiami areologicznymi. Zarządzanie Technologią, 6–14, Gorzów Wielkopolski – Poznań, **2014**.

[3] **Borkowski, J.**: Zużycie i trwaość ściernic, *PWN*, (in Polish), Warsaw **1990**.

[4] **Grzesik, W.**: Wpływ obróbki sekwencyjnej na topografi powierzchni stali utwardzonej, *Mechanik*, (in Polish), 5–6, p. 350–363, **2014**.

[5] **Grzesik, W., Rech, J. and Wanat, T.**: Surface finish on hardned bearing parts produced by superhard and abrasive tools, *International Journal Maching Tools Manufacture*, 47, pp.255–262, **2007**.

[6] **Grzesik, W.**: Szlifowanie ściernic CBN – charakterystyka profilu i topografii powierzchni utwardzonej stali po przeprowadzeniu procesu, cz.II, *Stal*, 5–6, p. 21–23, (in Polish), **2014**.

[7] **Oczoś, K. E.**: Doskonalenie techniki szlifowania. Część II, *Mechanik*, 10, (in Polish), **2005**.

[8] **Oczoś, K. E. and Liubimov, V.**: Struktura geometryczna powierzchni, (in Polish), Rzeszów, **2003**.

[9] **Rosik, R. and Grdulska, A.**: Wpływ prędkości szlifowania na stan warstwy wierzchniej w procesie szlifowania stopu tytanu, (in Polish), *Mechanik*, 8–9, p. 284–288, **2014**.

[10] **Wójcik, R.**: Nowe media i sposoby doprowadzenia do strefy szlifowania, *Archiwum Technologii Maszyn i Automatyzacji*, (in Polish), 28/4, 137–145, **2008**.

[11] **Wójcik, R. and Górecki, G.**: Modyfikacje ściernic do szlifowania w środowisku mgły olejowej, XXXII Naukowa Szkoła Obróbki Ściernej, (in Polish), 63–70, Koszalin – Darłowo, **2009**.

[12] http://www.htk.com.pl

[13] http:/universal–stal.pl

[14] http://www.ims–stalserwis.pl

[15] http://unionstal.pl